396 (1966).

[10] L. R. Windmiller, J. B. Ketterson, and S. Hornfeldt, Phys. Rev. B 3, 4213 (1971).

[11] F. M. Mueller, A. J. Freeman, J. O. Dimmock, and A. M. Furdyna, Phys. Rev. B 1, 4617 (1970).

[12] F. E. Hoare and B. Yates, Proc. Roy. Soc. (London) A240, 42 (1957).

[13] See, J. R. Schrieffer, J. Appl. Phys. 39, 642 (1968).

[14] E. Fawcett, E. Bucher, W. F. Brinkman, and J. P. Maita, Phys. Rev. Letters 21, 1183 (1968).

[15] Some work has been done on the effect of hydrostatic pressure on the magnetic moment of *ferromagnetic* Pd : Ni alloys. See, H. Fujiwara, N. Tsukiji, N. Yamate, and E. Tatsumoto, J. Phys. Soc. Japan 23, 1176 (1967).

[16] For the original calculation of the dynamical susceptibility $\chi(k, \omega)$ applicable to pure Pd see, T. Izuyama, D. J. Kim, and R. Kubo, J. Phys. Soc. Japan 18, 1025 (1963).

[17] J. Mathon, Proc. Roy. Soc. (London) A306, 355 (1968).

[18] J. G. Collins and G. K. White, in *Progress in Low-Temperature Physics*, edited by C. J. Gorter (North-Holland, Amsterdam, 1964), Vol. IV.

[19] This is an approximate value for the compressibility of Pd at room temperature. The compressibility at 0 °K should not be much changed since the bulk modulus $[V^{-1} \times (\partial V/\partial p)]^{-1}$ depends on the total free energy, and the contribution of excited states to the total free energy is small.

[20] H. F. Sterling and R. W. Warren, Metallurgia 67, 301 (1963).

[21] R. A. Beyerlein, thesis (University of Illinois, Urbana-Champaign, 1972) (unpublished).

[22] The four- (Cu) conductor swaged tubing was supplied by Continental Sensing, Inc. This firm has since gone out of business. A similar product may be obtained from American-Standard, Aeroresearch Dept., 9000 King St., Franklin Park, Ill. 60131.

[23] Epoxi-Patch Kit No. 6c, Aluminum Grey—supplied by the Dexter Corp., Hysol Division, Olean, N. Y. 14760.

[24] There was always more noise (~±4–6 nV) present in the low-temperature measurements.

[25] Room-temperature tests showed the bursting pressure of this tubing (Superior Tube Co., 1938 Germantown Ave., Norristown, Pa. 19404) to be 105 000 psi.

[26] W. D. Seward, D. Lazarus, and S. C. Fain, Jr., Phys. Rev. 178, 345 (1969).

[27] Heise Bourdon Tube Co., Inc., Newtown, Conn. 06470.

[28] J. S. Dugdale, Nuovo Cimento Suppl. 9, 27 (1958).

[29] J. T. Schriempf, Phys. Rev. Letters 20, 1034 (1968).

[30] P. W. Bridgman, *Physics of High Pressures* (G Bell, London, 1949), p. 160.

[31] N. D. Lang and H. Ehrenreich, Phys. Rev. 168, 605 (1968).

PHYSICAL REVIEW B VOLUME 7, NUMBER 1 1 JANUARY 1973

Effect of Crystal Fields on the Magnetic Properties of Samarium Intermetallic Compounds

H. W. de Wijn
Fysisch Laboratorium der Rijksuniversiteit van Utrecht, Utrecht, The Netherlands
and
A. M. van Diepen and K. H. J. Buschow
Philips Research Laboratories, Eindhoven, The Netherlands

(Received 27 July 1972)

Neither of the intermetallics $SmAl_2$ (a ferromagnet below $T_C = 120$ K) and $SmSn_3$ (an antiferromagnet below $T_N = 11$ K) show the sign reversal predicted by White and Van Vleck for the $4f$-induced Knight shift in the paramagnetic region. On the other hand, no particular anomaly has been observed in the temperature dependence of the susceptibility. An explanation for this is given in terms of mixing of excited J levels of Sm^{3+} into the $J = \frac{5}{2}$ ground multiplet by cubic crystal fields. The calculation is described of the crystal field matrix elements of Sm^{3+} between any J and J', and expressions are derived for the Knight shift and the susceptibility in the presence of crystalline and molecular fields. It is shown that the sixth-order component of the crystal field is important, and that the anomalous behavior is enhanced by ferromagnetic exchange between the Sm ions. A study of the lattice constants and the ^{27}Al quadrupolar coupling in comparison with other RAl_2 (R = rare earth) compounds excludes the possibility of Sm in $SmAl_2$ not being trivalent.

I. INTRODUCTION

In rare-earth intermetallic compounds the orbital as well as the spin part of the localized $4f$ magnetism is accessible to experimental study. In the paramagnetic region, the $4f$ magnetic susceptibility χ_f is a direct measure for the rare-earth magnetic moment, i.e., $\langle L_z + 2S_z \rangle$, while the part of the Knight shift at a nonmagnetic site due to s-f exchange enhancement of the conduction-electron-spin polarization K_f is proportional to $\langle S_z \rangle$. Within the ground multiplet of the rare earth, $\langle L_z + 2S_z \rangle$ and $\langle S_z \rangle$ are proportional to each other, differing by a factor $(g_f - 1)/g_f$, with g_f the Landé g factor.

Then, there is a linear relationship between K_f and χ_f with a slope proportional to a phenomenological s-f exchange constant $\mathcal{J}_{sf}$; and both quantities as a function of the temperature follow a Curie–Weiss law. For the first half of the series of tripositive rare-earth ions, where $J = L - S$, the $4f$ spins are polarized in the direction of the external magnetic field, whereas in the second half, where $J = L + S$, and for Gd^{3+}, which has $J = S$, the $4f$ spin polarization is in the opposite direction, so that the sign of K_f reverses in going through the rare earths. Experiments in several series of rare-earth intermetallics have largely confirmed these rules, while $\mathcal{J}_{sf}$ appeared to be fairly constant within a series (for a review see Refs. 1 and 2).

In the case of Sm^{3+}, however, the energy separation between the ground ($J = \frac{5}{2}$) and first excited ($J = \frac{7}{2}$) multiplets is only 1400 K, so that temperature-independent terms of the Van Vleck type are expected to contribute, although differently, to both susceptibility and Knight shift. In addition, the g factor of the ground multiplet of Sm^{3+} is only $\frac{2}{7}$, so that the Curie part of the susceptibility is small. As a result the linear relation between K_f and χ_f is lost. White and Van Vleck[3] have shown that the Van Vleck and Curie parts of the Knight shift are of the opposite sign, resulting in a sign reversal of K_f at a crossover temperature T_{co} of about 300 K. A more complete description, including contributions from excited multiplets populated mainly at elevated temperatures, could well account for the experimental data in $SmAl_3$,[4] with $T_{co} = 310 \pm 20$ K and $\mathcal{J}_{sf} = -0.21$ eV, the latter being equal to those found for the other RAl_3 (R = rare earth) compounds. Here, Sm^{3+} was essentially considered to be a free ion. White and Van Vleck already indicated that incorporation of a fourth-order only splitting *within* the ground state by crystal fields could result in a reduction of the crossover temperature. Jones and Hesse[5] have used such a crystal field splitting, along with readjustment of the mean-energy separation between $J = \frac{5}{2}$ and $J = \frac{7}{2}$, to describe their results in SmP, SmAs, SmSb, and SmBi. A slightly reduced crossover temperature has also been found in the case of $SmPt_2$.[6]

This simple model of the effects of crystal fields proved inadequate to account for a sign reversal of K_f occurring much below 300 K, or for a complete absence of the sign reversal. The latter situation has been observed in $SmSn_3$ by Borsa *et al.*[7] and in $SmAl_2$ by the present authors.[8] In these compounds K_f decreases towards lower temperatures without going through zero. The sign of the Van Vleck–type part of K_f is negative, in accord with the White–Van Vleck model; but the Curie part, apparently also negative, is opposite to what is expected for an $L - S$ ion. The present authors have previously suggested[8] that this anomalous behavior could be the result of mixing of excited multiplets into the ground state in the presence of crystal fields. Recently, Malik and Vijayaraghavan[9] showed that the crossover of K_f can indeed be suppressed when, in addition to the crystal field splitting within the $J = \frac{5}{2}$ ground multiplet, crystal-field-induced mixing of the $J = \frac{7}{2}$ multiplet into the ground state is allowed for. They restricted their treatment to fourth-order crystal fields, and as a result were not able to arrive at a crystal field parameter for which the calculated K_f and χ_f simultaneously fitted experiment. Further, an overall splitting of the ground state of about 500 K, a good fraction of the distance to the $J = \frac{7}{2}$ level, was needed to produce the effect. In view of this, it is questionable whether neglecting the crystal field splitting within the $J = \frac{7}{2}$ level is justified.

In the present investigation the effects of both fourth- and sixth-order crystal field potentials will be considered, with inclusion of all matrix elements within and in between at least the lowest three J multiplets. In addition, the perturbing effect of f-f exchange interaction of either sign will be considered. The model calculation will be compared with experimental data for the ferromagnetic $SmAl_2$ ($T_C = 120$ K) and the antiferromagnetic $SmSn_3$ ($T_N = 11$ K).

II. EXPERIMENTAL

A. Preparation and Crystal Structures

The samples of $SmAl_2$ and $SmSn_3$ were prepared by arc melting of the appropriate amounts of the constituent metals in an argon atmosphere. The samarium metal was 99.9% pure, aluminum and tin 99.99%. The samples were placed in a sintered Al_2O_3 crucible and annealed in vacuum at about 800 °C for three weeks. It was shown by x-ray diffraction that the samples were free of any second phase after annealing of the ingots. The samples were crushed to fine powders for the nuclear-magnetic-resonance (NMR) and susceptibility measurements.

The crystallographic structures of both $SmAl_2$ and $SmSn_3$ are cubic. $SmAl_2$ has the cubic Laves phase structure,[10] with a lattice constant $a = 7.945$ Å, and eight formula units $SmAl_2$ per unit cell. Each Sm ion is surrounded by a cubic coordination of 12 nearest-neighbor Al ions at $\frac{1}{8} a\sqrt{11}$ and four Sm ions at $\frac{1}{2} a\sqrt{3}$. Each Al is at a site of trigonal symmetry with six Al nearest neighbors and six Sm ions at a larger distance. $SmSn_3$ has the cubic Cu_3Au structure[11] with the Sm site at the corners of the cube and the Sn site at the centers of the faces. The lattice constant is $a = 4.684$ Å.

The lattice constants of both compounds fit in the monotonic variation of the lattice constants in going through the corresponding series of rare-earth intermetallics, from which it is concluded that the Sm ions are trivalent positive. For the RAl_2 compounds this is shown in Fig. 1. The lattice parameters of $EuAl_2$ and $YbAl_2$, in which Eu and Yb are divalent, behave in a way distinctively different from the lanthanide contraction of the RAl_2 compounds with trivalent rare earths. Further evidence for the trivalency of Sm in $SmAl_2$ is supplied by the variation of the nuclear quadrupole coupling through the series (see Sec. II C).

B. Susceptibility Measurements

The measurements of the susceptibilities were performed between 4.2 and 850 K with a Curie balance and, by employing the Faraday method, with a null-coil pendulum magnetometer. For the measurements above 300 K, the powders were sealed in evacuated silica tubes to prevent oxidation by air. Experimental values of the susceptibility of $SmAl_2$ in the paramagnetic region are plotted versus the temperature in Fig. 2. The ferromagnetic transition temperature, as determined from the temperature dependence of the magnetization, is 120 K, which is close to the value of Williams *et al.*[12] and also is in accord with resistivity data.[13] The magnetic moment per ion at 2 K is shown as a function of the applied field in the insert of Fig. 2. It is seen that $SmAl_2$ possesses a relatively high coercive force. The magnetic moment at 30 kG ($0.19\mu_B$) is roughly one-fourth of the free-ion value ($0.71\mu_B$), and is still increasing slightly with field. Possible causes for the lack of saturation at high fields are magnetic anisotropy and second-order Zeeman effect, contributions which cannot be separated experimentally. For a powder of spherical particles oriented at random the coercive force is $H_c = 0.64K_1/M$ (neglecting terms with K_2), while the maximum coercive force is $H_c' = 2K_1/M$. With $H_c \approx 6$ kG and $H_A = H_c'$ this gives a lower limit for the crystalline anisotropy field of about 18 kG. The results of measurements of the susceptibility of $SmSn_3$ are given in Fig. 3. This compound orders antiferromagnetically at 11 K. The susceptibilities in the region 4.2–300 K reported earlier by Tsuchida and Wallace[14] are a few percent lower than the present values. They observed a Néel temperature of 12 K.

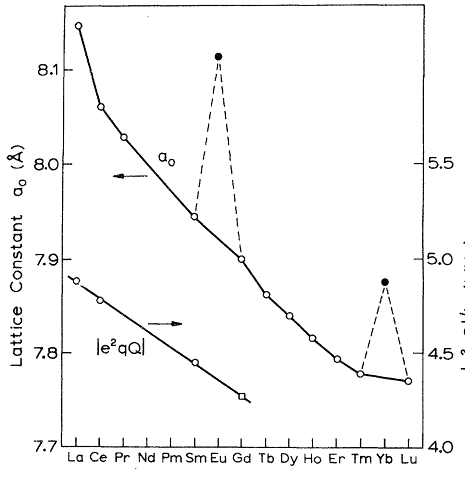

FIG. 1. Lattice parameters and ^{27}Al nuclear quadrupole coupling constants for the compounds RAl_2 at room temperature. The quadrupole coupling constant of $GdAl_2$ (open square) has been taken from Ref. 20.

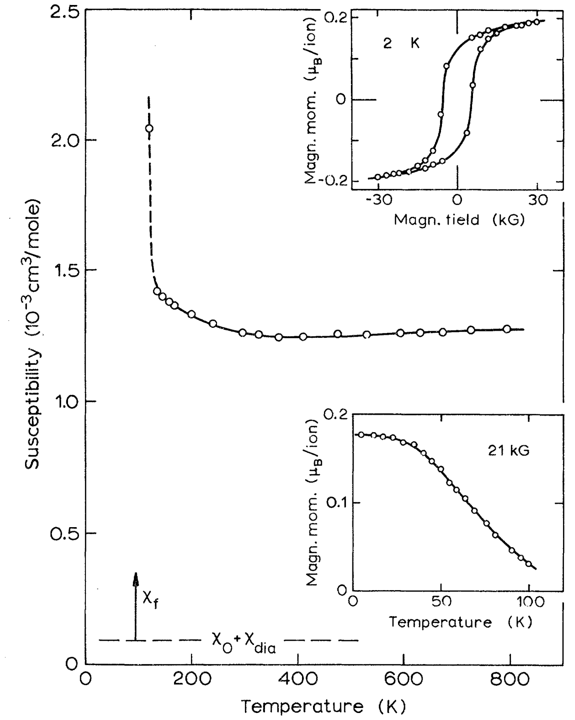

FIG. 2. Magnetic susceptibility χ of $SmAl_2$ versus the temperature. The upper insert shows the hysteresis loop at 2 K, while the lower insert gives the magnetization versus temperature in an applied field of 21 kG.

The total susceptibility at a temperature T may be written as

$$\chi(T) = \chi_f(T) + \chi_0 + \chi_{dia} . \qquad (1)$$

The Pauli susceptibility χ_0 and the diamagnetic susceptibility χ_{dia} are small relative to the $4f$-electron susceptibility χ_f. Their sum has been estimated by measuring the susceptibility at 300 K of the nonmagnetic compounds $LaAl_2$ and $LaSn_3$, respectively, with the result $\chi_0 + \chi_{dia} = +0.09\times10^{-3}$ cm^3/mole for $LaAl_2$, and $\chi_0 + \chi_{dia} = +0.15\times10^{-3}$ cm^3/mole for $LaSn_3$.

C. NMR Measurements

The NMR of the ^{27}Al nucleus ($I=\frac{5}{2}$, 100% abundant) has been examined in the paramagnetic re-

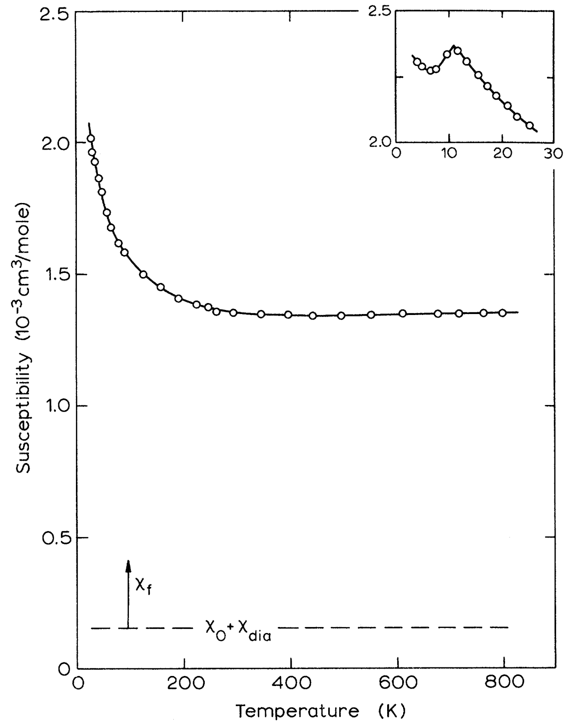

FIG. 3. Magnetic susceptibility χ of $SmSn_3$ versus the temperature. The insert shows the susceptibility near the Néel point with the temperature scale enlarged.

gion of $SmAl_2$, from 150 to 400 K, with a crossed-coils induction spectrometer operating at 5 MHz. The ^{27}Al resonance in the nonmagnetic solid $AlCl_3$ was taken as a reference to determine the Knight shifts. The experimental Knight shifts[8] are given in Fig. 4 as a function of the temperature. The Knight shift from Pauli paramagnetism only has been measured in the compound $LaAl_2$, isostructural with $SmAl_2$, and found to be $K_0 = +0.075\%$, while Barnes and Jones[15] found $K_0 = +0.055\%$.

The Al nucleus in $SmAl_2$ is at a site of axial symmetry, so that a splitting of the NMR line due to nuclear quadrupole coupling is expected. First-order quadrupole effects give rise to a splitting into five components, the central line not being shifted. Second-order quadrupole effects split this central transition, but do not affect the distance between its first nearest satellites. The Knight shift K of purely magnetic origin[16] was determined from the central transition, with this second-order effect taken into account. The quadrupole coupling constants e^2qQ, as determined from the satellites in first order and the central transition in second order, are equal within the experimental errors, and found to be linearly dependent on the temperature,

$$e^2qQ = e^2q_0Q(1 + bT) , \qquad (2)$$

with $|e^2q_0Q| = 4.79 \pm 0.07$ MHz and $b = (-2.4 \pm 0.3) \times 10^{-4}\ K^{-1}$. These values of e^2qQ are close to the nuclear quadrupole coupling constants measured for other members of the RAl_2 series. Values at room temperature, obtained by us, are given in Fig. 1, and agree with literature.[17-20] These data again demonstrate that Sm in $SmAl_2$ is trivalent. The temperature dependence of the electric field gradient q originates from thermal vibrations of the lattice.[21] The vibrations making by far the largest contribution to b are the short-wave bending modes of the lattice, which produce the largest relative displacements of nearby lattice sites. Such modes are compatible with the observed value of b, both in sign and magnitude.[22] Another effect that possibly interferes with the line shape of the central transition is anisotropic Knight shift.[16] Analysis of the line shape of the central transition, and of the second-order quadrupole effect compared to the first-order splitting, indicates that in $SmAl_2$ the anisotropic Knight shift, if present, is less than the isotropic shifts.

The Knight shift of the ^{119}Sn nucleus ($I = \frac{1}{2}$, 8.6% abundant) in $SmSn_3$ has earlier been reported by Borsa *et al.*[7] and later also by Malik,[6] in the temperature region 77–300 K. The anisotropic Knight shift is reported to be absent.[7] Their isotropic Knight shifts are reproduced in Fig. 4, together with one additional point measured by us at 300 K and 8 MHz. The Pauli Knight shift $K_0^{Sn} = +0.634\%$,

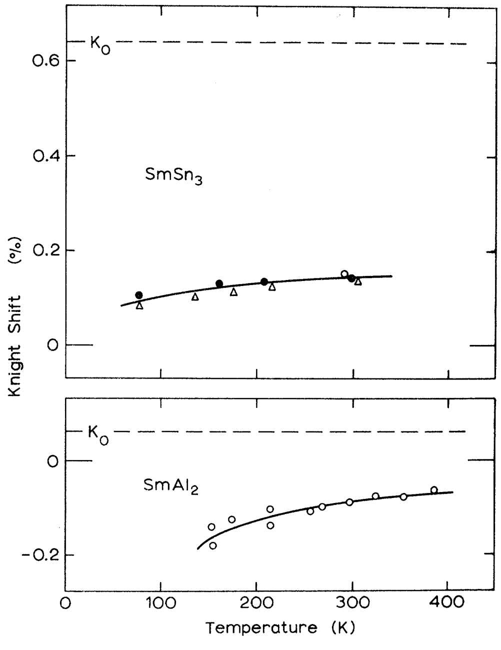

FIG. 4. Knight shift K of $SmAl_2$ and $SmSn_3$ versus the temperature. Our data are represented by open circles. The open triangles and black dots are data taken from Refs. 6 and 7, respectively.

obtained by Borsa *et al.*[7] from resonance in $LaSn_3$, is corroborated by our result of $+0.631\%$. The ^7Li NMR in an aqueous solution of LiCl was used as a reference with the assumption of $\nu(^7Li)/\nu(^{119}Sn) = 1.04285$.

III. THEORY

A. Crystal Field Matrix Elements

In this section we calculate the matrix elements in the *JM* representation of the crystal field Hamiltonian

$$\mathcal{H}_c = \sum_{k=0}^{\infty} \sum_{q=0}^{k} A_k^q \sum_i f_{kq}(\vec{r}_i) , \tag{3}$$

where the summation over i is carried over all the $4f$ electrons. The unrenormalized Tesseral harmonics f_{kq}, defined through

$$c_{k0} f_{k0}(\vec{r}) = r^k Y_k^0(\theta, \varphi) , \tag{4a}$$

$$c_{kq} f_{kq}(\vec{r}) = 2^{-1/2} r^k [Y_k^{-q}(\theta, \varphi) + (-1)^q Y_k^q(\theta, \varphi)] , \quad q > 0 \tag{4b}$$

along with their renormalization constants c_{kq}, are tabulated by Hutchings.[23] The summation over k in Eq. (3) may be restricted to $k \leq 6$, since otherwise the matrix elements are zero, while the term with A_0^0 is irrelevant. The point symmetry of the rare-earth site requires that a number of the lattice coefficients A_k^q vanish and that, for a certain k, and once the quantization axis (z axis) is chosen, the remaining A_k^q differ by constant factors. In the case of cubic symmetry, as in our problem, we have $A_4^4 = 5A_4^0 = 5A_4$ and $A_6^4 = -21A_6^0 = -21A_6$, when the z axis is chosen parallel to the [001] axis. Here, A_4 and A_6 are more general quantities describing the intensities of the fourth- and sixth-order ($k = 4, 6$) crystal fields irrespective of the direction of the z axis.

The standard approach to calculate the matrix elements of $\mathcal{H}_c$ in the *JM* representation is the method of the Stevens operator equivalents,[24,25] which provides the matrix elements through

$$\sum_i f_{kq}(\vec{r}_i) = \theta_k \langle r^k \rangle O_k^q , \tag{5}$$

where O_k^q are operators in terms of J_x, J_y, and J_z, while θ_k are multiplicative factors characteristic for the specific rare earth. A notation common in this context is $B_4 = A_4 \langle r^4 \rangle \theta_4$ and $B_6 = A_6 \langle r^6 \rangle \theta_6$. The method is used mainly for the calculation of matrix elements within the ground manifold of constant J, and has been extended to off-diagonal matrix elements between the ground J and $J+1$ states.[26,27]

However, since we wish to consider a more complete crystal field matrix, we turn to the direct calculation. The first step is taking apart the dependence on M by use of the Wigner–Eckart theorem. Second, the crystal field does not act on the spin, so that we may decouple the orbit from the spin. Collecting the effects of these two straightforward operations,[28] we arrive at

$$\begin{aligned} &\langle (4f)^n LS; JM | \sum_i r_i^k Y_k^q(\theta_i, \varphi_i) | (4f)^n LS; J'M' \rangle \\ &\quad = (-1)^{L+S-M+J-J'} [(2J+1)(2J'+1)]^{1/2} \\ &\qquad \times \begin{pmatrix} J & J' & k \\ -M & M' & q \end{pmatrix} \begin{Bmatrix} L & L & k \\ J & J' & S \end{Bmatrix} \langle L \| \sum_i r_i^k Y_k \| L \rangle , \end{aligned} \tag{6}$$

where the large parentheses and large curly brackets denote the Wigner $3j$ and $6j$ symbols, respectively. From the properties of these symbols it follows that the matrix elements obey the following selection rules and triangular conditions: $q = M - M'$, $|J - J'| \leq k \leq J + J'$, and $k \leq 2L$. The reduced matrix element $\langle L \| \sum_i r_i^k Y_k \| L \rangle$ has to be calculated by essentially the same technique (except for the decomposition of J) as the factors θ_k appearing in the Stevens formalism. In general, for the rare earth, $k \leq 6$. The result for Sm^{3+} ($n = 5$, $L = 5$) is

$$\langle L \| \sum_i r_i^4 Y_4 \| L \rangle = c_{40} \langle r^4 \rangle (2^9 \times 3^{-2} \times 11^{-1} \times 13)^{1/2} ,$$

$$\langle L \| \sum_i r_i^6 Y_6 \| L \rangle = -c_{60} \langle r^6 \rangle (2^{10} \times 3^{-3} \times 5^3 \times 11^{-1} \times 13^{-1} \times 17)^{1/2} .$$

A word should be said about the phase convention. While decomposing J in the derivation of Eq. (6), we have adopted the convention $\vec{J} = \vec{S} + \vec{L}$, with $\vec{S}$ the "first" and $\vec{L}$ the "second" operator. In doing so we have given the $\Delta J = \pm 1$ off-diagonal elements as derived from Eq. (6) the same sign as the corresponding elements in the Stevens operator equivalent language, Eq. (5). On the other hand, adopting $\vec{J} = \vec{L} + \vec{S}$ would have resulted in the opposite sign for the $\Delta J = \pm 1$ elements. Also, with the adopted phase convention the $\Delta J = \pm 1$ off-diagonal elements of $\vec{L}$ and $\vec{S}$ [cf. Eqs. (13) and (14)] are consistent with the standard definition, as used in Van Vleck's book[29] and in the Stevens formalism. For example, the elements $\langle J+1, M | S_z | J, M \rangle$ are positive.

In summary, solving the crystal field problem consists of diagonalizing the Hamiltonian

$$\mathcal{H} = \lambda \vec{L} \cdot \vec{S} + \mathcal{H}_c . \tag{7}$$

The matrix elements of the spin-orbit coupling are given by

$$\langle LS; JM | \lambda \vec{L} \cdot \vec{S} | LS; JM \rangle = \tfrac{1}{2} \lambda [J(J+1) - L(L+1) - S(S+1)] , \tag{8}$$

while the matrix elements of $\mathcal{H}_c$ are made up from Eqs. (4) and (6). For the $3j$ and $6j$ symbols we have used the tables by Rotenberg *et al.*[30] In particular, for a cubic field with $\vec{z} \parallel [001]$, Eq. (7) takes the form

$$\mathcal{H} = \lambda \vec{\mathrm{L}} \cdot \vec{\mathrm{S}} + A_4 \sum_i (f_{40} + 5f_{44}) + A_6 \sum_i (f_{60} - 21 f_{64}) , \tag{9}$$

where, for a given λ, we have two adjustable constants, viz., the crystal field parameters $A_4\langle r^4\rangle$ and $A_6\langle r^6\rangle$.

B. Knight Shift and Susceptibility

Having calculated the energy levels in a crystal field, we pass on to the calculation of Knight shifts and susceptibilities as a function of temperature in the paramagnetic region. The calculation, by use of perturbation theory up to second order, is a generalization of the derivation by White and Van Vleck[3] to include crystal and molecular fields.

The Knight shift resulting from the $4f$-induced polarization K_f is proportional to the net spin of the Sm^{3+} ion. That is, if K_0 is the Knight shift due to Pauli paramagnetism,

$$K_f(T) = K - K_0 = -K_0 \mathcal{J}_{sf} \langle S_z \rangle_{\mathrm{av}} / g_s \mu_B H , \tag{10}$$

where g_s (≈ 2) is the conduction-electron g value, $\mathcal{J}_{sf}$ is the phenomenological exchange constant between the $4f$ spins and the conduction-electron spins, and "av" denotes Boltzmann averaging over the crystal field levels of the Sm^{3+} ion. Similarly, the part of the magnetic susceptibility associated with the $4f$ electrons is

$$\chi_f(T) = -N\mu_B \langle L_z + 2S_z \rangle_{\mathrm{av}} / H . \tag{11}$$

In addition to the externally applied field H, the Sm ions are subject to an exchange field H_{ex}, which they exert on each other through the Ruderman–Kittel–Kasuya–Yosida mechanism.[31] In the paramagnetic region at $H \approx 10$ kG, H_{ex} is of the order of 1 kG or less, so that both fields may be treated as a perturbation. The total Zeeman Hamiltonian, perturbative on the crystal field problem [Eq. (7)], is thus[32]

$$\mathcal{H}_{\mathrm{pert}} = \mu_B H (L_z + 2S_z) + 2\mu_B H_{\mathrm{ex}} S_z , \tag{12}$$

where $L_z + 2S_z$ and S_z are given by [phase convention as in Eq. (6)]

$$\begin{aligned} &\langle JM | S_z | J'M' \rangle \\ &\quad = (-1)^{L+S-M} [(2J+1)(2J'+1)]^{1/2} \\ &\qquad \times \begin{pmatrix} J & J' & 1 \\ -M & M' & 0 \end{pmatrix} \begin{Bmatrix} S & S & 1 \\ J & J' & L \end{Bmatrix} [S(S+1)(2S+1)]^{1/2} , \end{aligned} \tag{13}$$

$$\begin{aligned} &\langle JM | L_z + 2S_z | J'M' \rangle \\ &\qquad = M \langle JM | J'M' \rangle + \langle JM | S_z | J'M' \rangle , \end{aligned} \tag{14}$$

with the selection rules $M = M'$ and $J - J' = 0, \pm 1$.

To incorporate the crystal field we first transform S_z and $L_z + 2S_z$ to the representation based on the eigenfunctions $|m\rangle$ of the crystal field levels by use of the transformation matrix $\langle JM | m \rangle$, already obtained in the diagonalization of the crystal field problem. We then proceed by calculating the expectation values $\langle S_z \rangle$ and $\langle L_z + 2S_z \rangle$ of each level by perturbation theory up to the second order,[33] and subsequent Boltzmann averaging of the expectation values over the crystal field levels and Zeeman sublevels. Retaining only terms linear in H and H_{ex}, we obtain Curie-type terms inversely proportional to the temperature and Van Vleck-type terms independent of the temperature.[29] In formulas,

$$\langle S_z \rangle_{\mathrm{av}} = \mu_B H \sigma_{L+2S,S} + 2\mu_B H_{\mathrm{ex}} \sigma_{S,S} , \tag{15}$$

$$\langle L_z + 2S_z \rangle_{\mathrm{av}} = \mu_B H \sigma_{L+2S,L+2S} + 2\mu_B H_{\mathrm{ex}} \sigma_{S,L+2S} , \tag{16}$$

in which we have abbreviated the summations over the crystal field levels m by use of

$$\begin{aligned} \sigma_{A,B} = \sigma_{B,A} = \sum_m \biggl(&-\frac{\langle m | A_z | m \rangle \langle m | B_z | m \rangle}{kT} \\ &+ 2 \sum_{m' \neq m} \frac{\langle m | A_z | m' \rangle \langle m' | B_z | m \rangle}{E_m^{(0)} - E_{m'}^{(0)}} \biggr) p_m^{(0)} , \end{aligned} \tag{17}$$

with $p_m^{(0)} = Z^{-1} \exp(-E_m^{(0)}/kT)$ the statistical weight of the unperturbed crystal field level $E_m^{(0)}$. To eliminate H_{ex} we substitute the molecular field[34]

$$2\mu_B H_{\mathrm{ex}} = -\mathcal{J}_{ff} \langle S_z \rangle_{\mathrm{av}} , \tag{18}$$

and obtain the final expressions for the Knight shift and susceptibility, which are to be used in Sec. IV:

$$\frac{\langle S_z \rangle_{\mathrm{av}}}{\mu_B H} = \frac{\sigma_{L+2S,S}}{1 + \mathcal{J}_{ff} \sigma_{S,S}} , \tag{19}$$

$$\frac{\langle L_z + 2S_z \rangle_{\mathrm{av}}}{\mu_B H} = \sigma_{L+2S,L+2S} - \mathcal{J}_{ff} \frac{(\sigma_{L+2S,S})^2}{1 + \mathcal{J}_{ff} \sigma_{S,S}} . \tag{20}$$

IV. DISCUSSION

A. Numerical Results

By use of the framework presented in Sec. III, the Knight shift $K_f = K - K_0$ and the susceptibility χ_f have been calculated as a function of the temperature for a wide range of values of the crystal field parameters $A_4\langle r^4\rangle$ and $A_6\langle r^6\rangle$. The calculated $K_f(T)$ and $\chi_f(T)$ have subsequently been compared with the experimental data given in Figs. 2–4. Agreement between theory and experiment could only be obtained for a limited number of sets of $A_4\langle r^4\rangle$ and $A_6\langle r^6\rangle$, which are indicated in Fig. 5 by the shaded areas. For the ferromagnetic compound $\mathrm{SmAl_2}$, the expectation value of $\langle L_z + 2S_z \rangle$ of the lowest level is in accord with the moment observed in high fields at 2 K (see insert to Fig. 2).

In these calculations, $\mathcal{J}_{ff}$ for the ferromagnet $\mathrm{SmAl_2}$ has been chosen such as to yield divergence of χ_f at an asymptotic Curie temperature θ_p equated to the observed $T_C = 120$ K with the molecular-field relation $\theta_p = T_C$. The result appears to be only weakly dependent on the crystal field parameters,

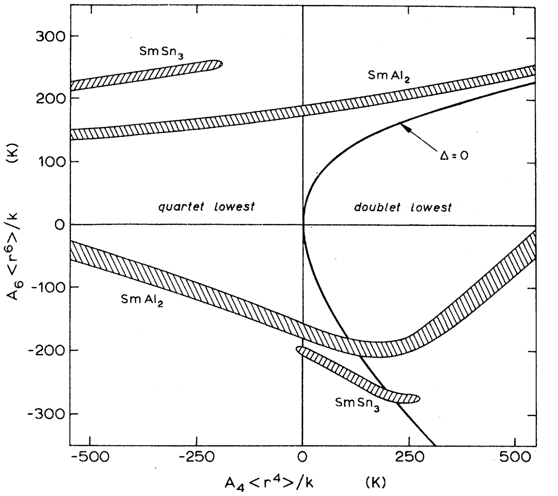

FIG. 5. Crystal field parameters $A_4\langle r^4\rangle$ and $A_6\langle r^6\rangle$ for Sm^{3+} in $SmAl_2$ and $SmSn_3$. For the combinations lying in the shaded areas Knight shift and susceptibility could simultaneously be fitted to experiment. Combinations for which the doublet and quartet originating from the $J=\frac{5}{2}$ multiplet accidentally coincide are indicated by the curve $\Delta=0$.

and we have therefore adopted $\mathcal{J}_{ff}/k=70$ K throughout. It is of interest to note that the relation $k\theta_p=\frac{1}{3}\mathcal{J}_{ff}(g_f-1)^2J(J+1)$, whose validity is restricted to the rare earths in which only the ground J multiplet is involved, would yield $\theta_p=104$ K for $\mathcal{J}_{ff}/k=70$ K, the difference being due to mixing of higher multiplets into the $J=\frac{5}{2}$. Unfortunately, in the case of $SmSn_3$, which orders antiferromagnetically, θ_p cannot be evaluated from a molecular-field relation. To estimate $\mathcal{J}_{ff}$ for $SmSn_3$ we have therefore scaled the value for $SmAl_2$ with the ratio of the paramagnetic Curie temperatures of other RSn_3 compounds[7, 14] and those of the corresponding RAl_2 compounds,[12] which yields $J_{ff}/k=-25$ K. In all calculations the spin-orbit coupling was taken to be $\lambda/k=410$ K, the value that successfully explained the crossover of the Knight shift in $SmAl_3$ at 310 K.[4]

Through Eq. (10) the fitting of theory to experiment yields the product $K_0\mathcal{J}_{sf}$. For $SmAl_2$, $K_0\mathcal{J}_{sf}$ varies with the location in the shaded areas of Fig. 5 between -0.011 and -0.016, and for $SmSn_3$ between -0.06 and -0.09, where K_0 and $\mathcal{J}_{sf}$ are expressed in percent and eV, respectively. For $SmAl_2$ with $K_0\approx 0.06\%$, there follows $\mathcal{J}_{sf}\approx -0.23$ eV, which is in excellent accord with the values of -0.2 to -0.3 eV found from Knight-shift measurements in other RAl_2 compounds.[17–20] For $SmSn_3$ with $K_0\approx 0.63\%$, $\mathcal{J}_{sf}\approx -0.12$ eV, while in the other RSn_3 compounds an average of -0.08 eV has been reported.[7]

To show the general characteristics of the dependence on the parameters $A_4\langle r^4\rangle$, $A_6\langle r^6\rangle$, and $\mathcal{J}_{ff}$ we present some examples of the calculated $K_f(T)$ and $\chi_f(T)$ for the case of $SmAl_2$. In Fig. 6 we first show the dependence of K_f on $A_6\langle r^6\rangle$, with the fourth-order crystal field and the f-f exchange kept fixed (solid curves). The curve for $A_4\langle r^4\rangle/k=+350$ K and $A_6\langle r^6\rangle/k=-140$ K corresponds to a possible point on the lower branch of Fig. 5 and agrees with the experimental data (Fig. 4), whereas the other curves shown deviate appreciably from experiment. Upon removing the sixth-order field the Knight shift increases and eventually changes sign in the temperature region below, say, 300 K, thus recovering the crossover in the temperature-dependence characteristic for the White–Van Vleck theory. A similar behavior is found when $A_4\langle r^4\rangle$ instead of $A_6\langle r^6\rangle$ is varied (broken curves in Fig. 6). In Fig. 7 we give the curve in the case $A_4\langle r^4\rangle/k=+150$ K and $A_6\langle r^6\rangle/k=-200$ K, another possibility located on the lower branch in Fig. 5, and vary $\mathcal{J}_{ff}$, keeping the crystal field parameters fixed. It is seen that a ferromagnetic exchange field has a pronounced effect, and if sufficiently strong, i.e., θ_p being of the order of or greater than T_{co}, removes the sign reversal of $K_f(T)$. In general, the effect of a variation of the quantities $A_4\langle r^4\rangle$, $A_6\langle r^6\rangle$, and $\mathcal{J}_{ff}$ is less pronounced in the case of $\chi_f(T)$. We therefore confine ourselves to showing an example of the dependence on the parameter $A_6\langle r^6\rangle$ (Fig. 8). We finally note that the dependence of $K_f(T)$ and $\chi_f(T)$ on the crystal field parameters and $\mathcal{J}_{ff}$ varies from site to site on the

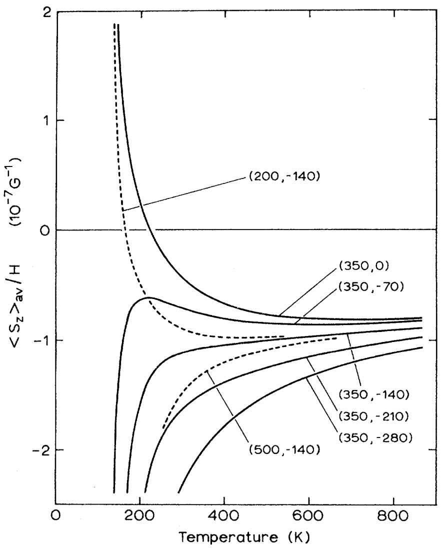

FIG. 6. Effect of variation of $A_6\langle r^6\rangle$ (solid curves) and $A_4\langle r^4\rangle$ (broken curves) on $\langle S_z\rangle_{av}/H$ for Sm^{3+} in a cubic crystal field. The numbers in parentheses are the values for $A_4\langle r^4\rangle/k$ and $A_6\langle r^6\rangle/k$ in kelvin, respectively. For $\mathcal{J}_{ff}/k$ the value for $SmAl_2$, $\mathcal{J}_{ff}/k=+70$ K, is used.

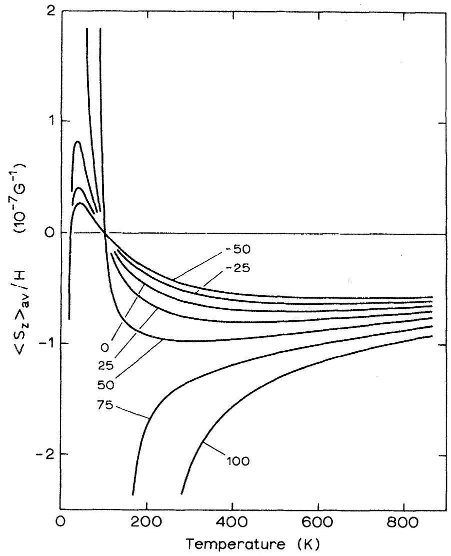

FIG. 7. Effect of different exchange fields on $\langle S_z\rangle_{av}/H$ for Sm^{3+} in a cubic crystalline field with $A_4\langle r^4\rangle/k=+150$ K and $A_6\langle r^6\rangle/k=-200$ K. The curves are labeled with the values for $\mathcal{J}_{ff}/k$ in kelvin.

branches in Fig. 5 and may be quite different in appearance from the examples we have given here.

B. Variations of Model

In Sec. IV A we studied the effect of crystal fields on the Knight shift and susceptibility, making use of the crystal field matrix, including all elements diagonal and off diagonal in J, and the spin-orbit coupling matrix for the five lowest multiplet levels [$J=\frac{5}{2}$ up to $\frac{13}{2}$ inclusive; cf. case (a) below], or, if sufficiently accurate, for the three lowest levels [$J=\frac{5}{2}$, $\frac{7}{2}$, and $\frac{9}{2}$; cf. case (b) below]. In the present section we truncate the full five-level matrix step by step in order to find out which part of the crystal field matrix is responsible for the major contribution to the anomalous behavior.

The Knight shift and susceptibility are presented as the curves marked (a) in Figs. 9 and 10, respectively, for the full five-multiplet-level Hamiltonian for $A_4\langle r^4\rangle/k=+350$ K, $A_6\langle r^6\rangle/k=-140$ K, and $\mathcal{J}_{ff}/k=+70$ K, a possible combination for $SmAl_2$. In curves (b) similar results are given for the full three-multiplet Hamiltonian. Below, say, 250 K, (b) shows no appreciable deviations from (a). At higher temperatures there are small variations, generally less than the experimental uncertainties, indicating that the three-level scheme is usually sufficiently accurate for our purposes. Curves (c) apply to the full two-level matrix, i.e., including all crystal field elements within $J=\frac{5}{2}$ and $\frac{7}{2}$, and all off-diagonal elements between $\frac{7}{2}$ and $\frac{5}{2}$, and spin orbit up to $J=\frac{7}{2}$. They represent a continuation of the trend encountered in going from (a) to (b). The deviations, however, now lie far outside the experimental errors. In particular, the susceptibility has lost its characteristic shallow minimum around 350 K. In case (d) we have fur-

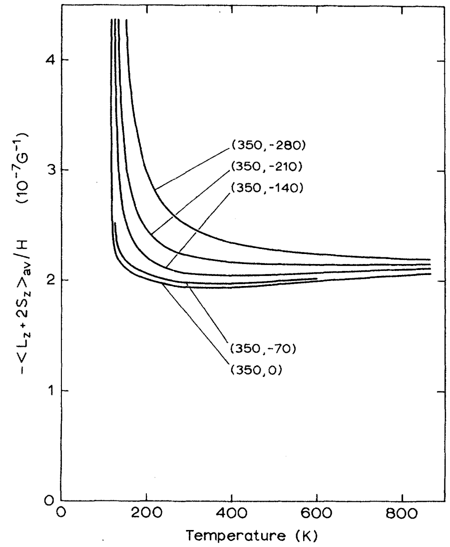

FIG. 8. Effect of variation of $A_6\langle r^6\rangle$ on $-\langle L_z+2S_z\rangle_{av}/H$ for Sm^{3+} in a cubic crystal field. The numbers in parentheses are the values for $A_4\langle r^4\rangle/k$ and $A_6\langle r^6\rangle/k$ in kelvin, respectively. For $\mathcal{J}_{ff}/k$ the value for $SmAl_2$, $\mathcal{J}_{ff}=+70$ K, is used.

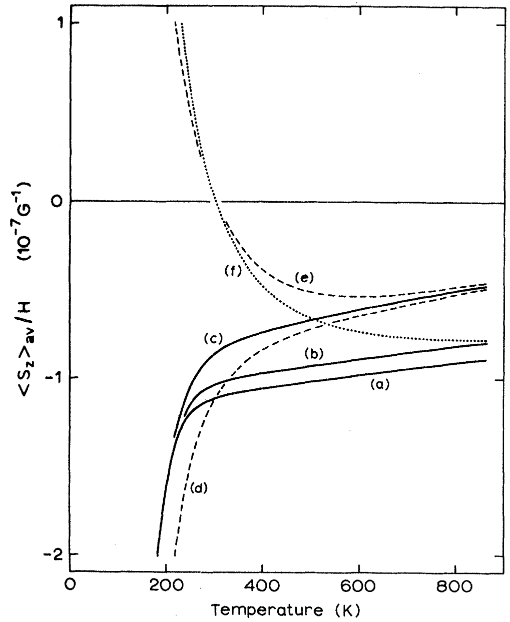

FIG. 9. Effect on $\langle S_z\rangle_{av}/H$ of step-by-step truncation of the crystal field matrix of Sm^{3+} in a cubic crystal field with $A_4\langle r^4\rangle/k=+350$ K and $A_6\langle r^6\rangle/k=-140$ K, while $\mathcal{J}_{ff}/k=+70$ K, as described in the text.

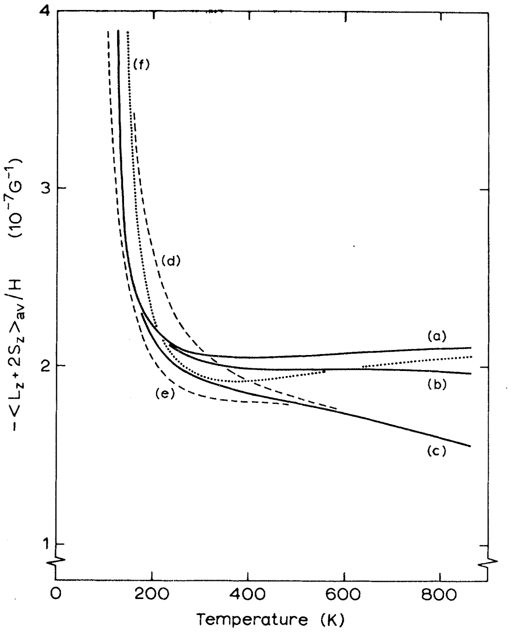

FIG. 10. Effect on $-\langle L_z+2S_z\rangle_{av}/H$ of step-by-step truncation of the crystal field matrix of Sm^{3+} in a cubic crystal field with $A_4\langle r^4\rangle/k=+350$ K and $A_6\langle r^6\rangle/k=-140$ K, while $\mathcal{J}_{ff}/k=+70$ K, as described in the text.

ther truncated the crystal field matrix by removing the $J=\frac{7}{2}$ diagonal elements. It is seen that the gross features of the temperature dependence are still preserved, but no adequate description of experiment is to be expected. This is, in fact, the model used by Malik and Vijayaraghavan[9] (except for the inclusion of sixth-order crystal fields and exchange interaction) to include "second-order crystal field effects."

Reducing the matrix still further, we take out the $J=\frac{7}{2}, \frac{5}{2}$ off-diagonal crystal field elements and obtain curves (e). Finally, for comparison, the results of the free-ion model, with the inclusion of all multiplet levels and with exchange taken into account, are given in curves (f). This is the model used in describing the Knight shift and susceptibility of $SmAl_3$,[4] and is an extension of White and Van Vleck's original treatment to explain the sign reversal of the $4f$ Knight shift at about 300 K by second-order Zeeman effects due to the $J=\frac{7}{2}$ multiplet level. White and Van Vleck also suggested that the effects of crystal fields on the Knight shift might possibly be described by inclusion of the $J=\frac{5}{2}$ ground-level splitting, as in curves (e).

To sum up, the major features of the anomalous behavior of the Knight shift encountered in $SmAl_2$ and $SmSn_3$ are explained by taking into account mixing of the $J=\frac{7}{2}$ and $\frac{5}{2}$ states by crystal fields, as in case (d). But for a calculation of sufficient accuracy to permit comparison with experiment, a more complete crystal field Hamiltonian matrix is required.

V. CONCLUDING REMARKS

It has been shown that crystal fields can explain the anomalous temperature dependence of the Knight shift in the intermetallic compounds $SmAl_2$ and $SmSn_3$, while at the same time being in accord with the $4f$ susceptibility. Also the values of the s-f exchange constant $\mathcal{J}_{sf}$ derived for $SmAl_2$ and $SmSn_3$ are, within the experimental uncertainties, in line with those found for the other members of the corresponding series of rare-earth intermetallic compounds. The effect of sixth-order crystal fields appeared to be significant, and their presence essential in the case of $SmSn_3$, while ferromagnetic exchange fields enhance the anomalous behavior.

Unfortunately, no unique solutions for the crystal field parameters have emerged in fitting the experiments. The *a priori* neglect of the sixth-order components of the crystal field relative to the fourth-order components, as is frequently done on the basis of simple point-charge calculations, has no experimental support in the literature, and also is in contradiction with our findings. An estimate for the crystal field splitting of the ground multiplet in $SmAl_2$ may be obtained from comparison with data on the crystal field splitting in $CeAl_2$. In the case of Ce^{3+} only the fourth-order component of the cubic crystal field is operative, splitting the $J=\frac{5}{2}$ level into a doublet and a quartet. It follows from specific-heat data[35] and resistivity data[36,37] that the distance between the doublet and the quartet in $CeAl_2$ is about 100 K, corresponding to $A_4\langle r^4\rangle/k\approx+45$ K. The entropy change involved in the antiferromagnetic-to-paramagnetic transition at 4 K shows that the doublet lies lowest.[38] These results indicate that in $SmAl_2$ the parameter $A_4\langle r^4\rangle$ is positive and of the order of several tens of kelvin. From Fig. 5 it then would follow that $A_6\langle r^6\rangle$ is of the order of 100–200 K, with the sign dependent on the branch.

An interesting conclusion of the present work, pertinent to metallic as well as insulating magnetic compounds of Sm with other magnetic ions, is that in the presence of suitable crystal fields a Sm^{3+} ion has a reversed sign of $\langle S_z\rangle$, i.e., acts as an $L+S$ ion instead of an $L-S$ ion. As a consequence of crystal fields, exchange interactions in which Sm^{3+} is involved unilaterally may apparently have changed from ferromagnetic to antiferromagnetic, or vice versa. This effect is unique for Sm^{3+}, since for the other tripositive rare earths, where only the ground J multiplet is relevant, crystal fields cannot change the ratio between the magnetic moment and $\langle S_z\rangle$.

[1] H. W. de Wijn, K. H. J. Buschow, and A. M. van Diepen, Phys. Status Solidi 30, 759 (1968).

[2] E. D. Jones, Phys. Rev. 180, 455 (1969).

[3] J. A. White and J. H. Van Vleck, Phys. Rev. Letters 6, 412 (1961).

[4] H. W. de Wijn, A. M. van Diepen, and K. H. J. Buschow, Phys. Rev. 161, 253 (1967). The second factor of Eq. (11) in text should read $[J^2-(S-L)^2]$. The calculations are based on the correct expression.

[5] E. D. Jones and J. E. Hesse, J. Appl. Phys. 38, 1159 (1967).

[6] S. K. Malik, Phys. Letters 31A, 33 (1970).

[7] F. Borsa, R. G. Barnes, and R. A. Reese, Phys. Status Solidi 19, 359 (1967).

[8] K. H. J. Buschow, A. M. van Diepen, and H. W. de Wijn, Phys. Letters 24A, 536 (1967).

[9] S. K. Malik and R. Vijayaraghavan, Phys. Letters 34A, 67 (1971); J. Phys. (Paris) 32 C1, 1028 (1971).

[10] J. H. Wernick and S. Geller, Trans. AIME 218, 866 (1960); S. E. Hasko, *ibid.* 218, 958 (1960).

[11] I. R. Harris and G. V. Raynor, J. Less-Common Metals 9, 7 (1965).

[12] H. J. Williams, J. H. Wernick, E. A. Nesbitt, and R. C. Sherwood, J. Phys. Soc. Japan 17BI, 91 (1962).

[13] H. J. van Daal and K. H. J. Buschow, Phys. Status Solidi (a) 3, 853 (1970).

[14] T. Tsuchida and W. E. Wallace, J. Chem. Phys. 43, 3811 (1965).

[15] R. G. Barnes and E. D. Jones, Solid State Commun. 5, 285 (1967).

[16] The combined effect of anisotropic magnetic shifts and quadrupole interactions on the line shape and position has been discussed in great detail by W. H. Jones, T. P. Graham, and R. G. Barnes, Phys. Rev. 132, 1898 (1963).

[17] V. Jaccarino, B. T. Matthias, M. Peter, H. Suhl, and J. H. Wernick, Phys. Rev. Letters 5, 251 (1960).

[18] R. G. Barnes, W. H. Jones, and T. P. Graham, Phys. Rev. Letters 6, 221 (1961).

[19] W. H. Jones, T. P. Graham, and R. G. Barnes, Phys. Rev. 132, 1898 (1963).

[20] E. D. Jones and J. I. Budnick, J. Appl. Phys. 37, 1250 (1966).

[21] T. Kushida, G. B. Benedek, and N. Bloembergen, Phys. Rev. 104, 1364 (1956).

[22] H. W. de Wijn and J. L. de Wildt, Phys. Rev. 150, 200 (1966).

[23] M. T. Hutchings, in *Solid State Physics*, edited by F. Seitz and D. Turnbull (Academic, New York, 1964), Vol. 16, p. 227ff.

[24] K. W. H. Stevens, Proc. Phys. Soc. (London) 65A, 209 (1952).

[25] A. Abragam and B. Bleaney, *Electron Paramagnetic Resonance of Transition Ions* (Clarendon, Oxford, 1970).

[26] R. J. Elliott and K. W. H. Stevens, Proc. Roy. Soc. (London) 218A, 553 (1953).

[27] B. R. Judd, Proc. Roy. Soc. (London) 227A, 552 (1964).

[28] A. R. Edmonds, *Angular Momentum in Quantum Mechanics* (Princeton U. P., Princeton, N. J., 1957).

[29] J. H. Van Vleck, *The Theory of Electric and Magnetic Susceptibilities* (Oxford U. P., Oxford, England, 1932).

[30] M. Rotenberg, R. Bivins, N. Metropolis, and J. K. Wooten, Jr., *The 3-j and 6-j Symbols* (MIT Press, Cambridge, Mass., 1959).

[31] M. A. Ruderman and C. Kittel, Phys. Rev. 96, 99 (1954); T. Kasuya, Progr. Theoret. Phys. (Kyoto) 16, 45 (1956); K. Yosida, Phys. Rev. 106, 893 (1957).

[32] It is no limitation to choose the external field parallel to the z axis, i.e., one of the cube axes [001]. The Knight shifts and susceptibilities are essentially the same if the external field were chosen for example along [111] or [011].

[33] In case the quantization axis is along [001] we can avoid the use of degenerate perturbation theory. Each submatrix of the factorized $\mathcal{H}_c$ matrix yields nondegenerate eigenvalues, while the perturbation does not have matrix elements outside the submatrices of $\mathcal{H}_c$.

[34] Note that $\mathcal{J}_{ff}$ in Ref. 4 differs from the present definition by a factor of 2.

[35] C. Deenadas, A. W. Thompson, R. S. Craig, and W. E. Wallace, J. Phys. Chem. Solids 32, 1853 (1971).

[36] H. J. van Daal and K. H. J. Buschow, in *Proceedings of the Colloque International des Elêments des Terres Rares, Paris-Grenoble*, 1969 (CNRS, Paris, 1970) p. 551.

[37] V. U. S. Rao and W. E. Wallace, Phys. Rev. B 2, 4613 (1970).

[38] R. W. Hill and J. M. Machado da Silva, Phys. Letters 30A, 13 (1969).